Available online at www.sciencedirect.com
ScienceDirect
Catalysis Today 133–135 (2008) 7–12
CATALYSIS TODAY
www.elsevier.com/locate/cattod

# Carbon nanofiber growth onto a cordierite monolith coated with Co-mordenite

M.A. Ulla [b,*], A. Valera [a], T. Ubieto [a], N. Latorre [a], E. Romeo [a], V.G. Milt [b], A. Monzón [a,*]

[a] *Instituto de Nanociencia de Aragón (INA), Universidad de Zaragoza, 50009 Zaragoza, Spain*
[b] *Instituto de Investigaciones en Catálisis y Petroquímica (INCAPE), (FIQ, UNL-CONICET), Santiago del Estero 2829, 3000 Santa Fe, Argentina*

Available online 3 January 2008

**Abstract**

The growth of carbon nanofibers (CNF) was studied over a cordierite monolith previously coated with mordenite synthesized by a hydrothermal route. The zeolitic layer was deposited in order to have the sufficient number of cationic exchange sites to anchor the metallic particles responsible for the CNF formation. To produce the carbon nanofibers, cobalt was the active metal and acetylene, the source of carbon. The amount and type of nanocarbonaceous material obtained were studied as a function of the following operating conditions: (i) the reduction temperature of the metallic phase, (ii) the presence or absence of $H_2$ in the feed and (iii) the orientation of the monolith channels with respect to the flow direction. The results obtained indicate that under specific operating conditions, large amounts of fibers grow over the whole internal surface of the channels. These fibers provide a large specific surface, which indicates that this type of structured catalysts could be used as three-phase reactors.


*Keywords:* CNF; Structured catalyst; Monolith

## 1. Introduction

The efficiency in catalytic three-phase reactions is mainly defined by the contact conditions between liquid and gas phases and solid catalysts. In general, two types of reactors are used for these processes, slurry and trickle-bed reactors. However, there are some reaction conditions where they present important mass transfer limitations and subsequent separation operations for recovering the solid catalyst [1]. In these cases, structured reactors seem more appropriate. The main advantages of these reactors are, among others, large liquid–solid surface area, no need of a subsequent separation operation, low pressure drop and decoupling of extraparticle–intraparticle distances [2].

Monolith and foam structures usually have a large geometric area but small specific surface area. Therefore, if the monolith walls are coated with carbon nanofibers (CNF), the surface area could increase in hundreds of square meters.

There are different methods to produce CNF; one of them is via decomposition of a gaseous component containing carbon such as $CH_4$ and $C_2H_2$ over small metallic particles ($Co^0$, $Ni^0$, and $Fe^0$). The primary structure and the dimensions of the obtained nanofibers depend on the reaction temperature, the reacting stream composition, the size and distribution of the metal particles, the active metal and the support.

In this work we study the growth of carbon nanofibers (CNF) over a cordierite monolith previously coated with mordenite, synthesized by a hydrothermal route [3]. The zeolitic layer was deposited in order to have the sufficient number of cationic exchange sites to anchor the metallic particles responsible for the CNF formation. To produce the carbon nanofibers, cobalt was the active metal and acetylene, the source of carbon.

* Corresponding author.
*E-mail addresses:* mulla@fiqus.unl.edu.ar (M.A. Ulla), amonzon@unizar.es (A. Monzón).

0920-5861/$ – see front matter © 2007 Elsevier B.V. All rights reserved.
doi:10.1016/j.cattod.2007.11.026

## 2. Experimental

### 2.1. Development of Co-mordenite coating onto the cordierite monolith (Co-Mor/Cor)

Substrates of 1 cm × 1 cm × 0.5 cm dimensions were obtained by cutting a cordierite honeycomb monolith (Corning, 400 cpsi). Before the coating procedure, the substrates were washed, dried at 120 °C and the external walls were wrapped with teflon ribbon. The mordenite coating on these substrates was produced by hydrothermal synthesis after seeding the monolith walls. Synthesis method details were previously described [3]. Briefly, the seeding was done by dip-coating the substrates into a 20 g $l^{-1}$ suspension of mordenite seeds for 30 s. The hydrothermal synthesis of the mordenite coating on seeded substrates took place in a teflon-lined autoclave at 180 °C for 24 h, using a gel with the following molar composition: $H_2O:SiO_2:Na_2O:Al_2O_3 = 80:1:0.38:0.025$. After the synthesis, mordenite coated substrates (Mor/Cor) were washed and treated in an ultrasonic bath for 10 min to remove the possible loose crystals deposited on the surface. The cobalt exchange was done using a 0.025 M $Co(CH_3COO)_2$ solution at 25 °C for 16 h and then at 60 °C for 8 h (Co-Mor/Cor).

### 2.2. Carbon nanofiber (CNF) growth onto Co-Mor/Cor

The CNF growth took place in a quartz microbalance in line with a continuous flow system under atmospheric pressure at 700 °C. This system also had a temperature-programmed controller and a mass flow controller. The standard atmospheric reactant mixture comprised $C_2H_2$ (5%) and $H_2$ (0 or 5%), balanced in $N_2$. The carbon production was determined by weight difference.

In order to analyze the effect of the monolith channel path with respect to the reacting flow direction on the CNF yield, the Co-Mor/Cor sample was held in the quartz microbalance with its channels positioned in two different ways: parallel and perpendicular to the gas flow direction.

So as to investigate the effect of the reduction prior to the CNF growth, some Co-Mor/Cor samples were reduced in diluted $H_2$ flow at two temperatures, 700 and 800 °C, in the same flow-system mentioned above.

### 2.3. Characterization

Mordenite and carbon nanofiber coating morphologies were examined by scanning electron microscopy (SEM) using a JEOL JSM 6400 instrument operated at 20 kV. The M/Al (M = Si, Co and Mg) ratio profiles were measured using an energy-dispersive X-ray analysis (EDX) system attached to the SEM instrument. X-ray diffraction patterns of the samples were obtained with a XD-D1 Shimadzu diffractometer operating at 30 kV and 40 mA. The scanning rate was 1° $min^{-1}$ and the $2\theta$ range from 5° to 50°.

The CNF coating was also characterized by transmission electron microscopy (TEM) and Raman spectroscopy. The TEM micrographs were obtained with a JEOL 2000 FX2 equipment operated at 200 kV and $2 \times 10^{-5}$ Pa. The Raman spectra were recorded using the TRS-600-SZ-P Jasco Laser Raman instrument equipped with a CCD (charge coupled device) with the detector cooled to about 153 K using liquid $N_2$. The excitation source was the 514.5 nm line of a Spectra 9000 Photometrics Ar ion laser, whereas the laser power was set at 30 mW.

Temperature-programmed reduction (TPR) was used to study the reducibility of the different cobalt species present on Co-Mor/Cor. The experiments were run on an Okhura TP-2002 S equipment with a TCD detector. The reducing gas flow was 5% $H_2$ in Ar and the heating rate, 10 °C $min^{-1}$.

## 3. Results and discussion

### 3.1. Co-Mor/Cor characterization

The signals observed on the XRD patterns of Co-Mor/Cor were consistent with the cordierite and mordenite phases. A SEM micrograph of this sample is shown in Fig. 1. The mordenite coating consisted of needle-shaped, well-developed crystals with low intergrowth. These characteristics enhanced the accessibility to each mordenite crystal [3]. The distribution of different components through the mordenite layer thickness was homogeneous, around 6 and 8 for Si/Al, and 0.3 and 0.4 for Co/Al. Magnesium was not found in the mordenite coating; consequently, no migration of this element from the cordierite wall to the zeolite layer was produced. However, the Si/Al ratio obtained for the zeolite layer was lower than that of the synthesis gel (Si/Al = 20) suggesting that the Al migration from the cordierite might have occurred during the synthesis procedure.

Fig. 2 shows the temperature-programmed reduction profile of Co-Mor/Cor. The reduction of $Co^{2+}$ located at the mordenite exchange sites occurs at high temperatures, around 820 °C, whereas the reduction procedure of highly dispersed $CoO_x$ and hydroxo-Co species starts at 600 °C. The latter species may be produced on the zeolite surface during either the ionic exchange procedure or the calcination treatment. The $Co_3O_4$ clusters

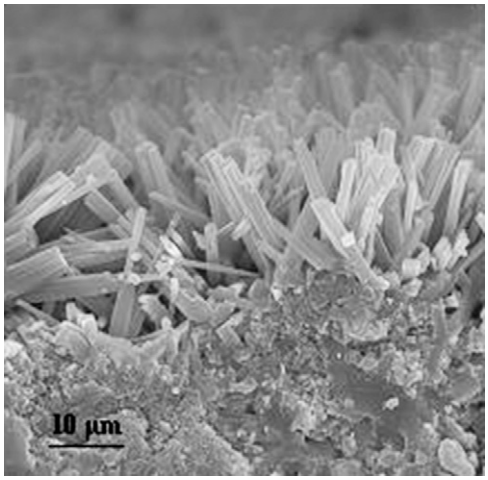


Fig. 1. Morphology of the Co-mordenite coating onto cordierite monolith.

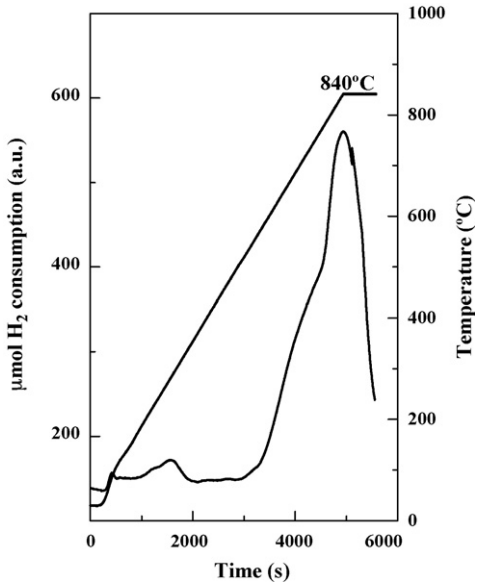


Fig. 2. Hydrogen consumption of Co-Mor/Cor (TPR).

reduction is expected to occur in the 250–450 °C temperature range [4,5]. Therefore, the reduction temperature of the different Co species presented on the mordenite coating has the following order:

$Co_3O_4$ (cluster) < $CoO_x$ and hydroxo

– Co species < $Co^{2+}$ in mordenite exchange sites.

### 3.2. Growth of carbon nanofiber (CNF) onto Co-Mor/Cor

Two samples of Co-Mor/Cor were reduced at different temperatures, 700 and 800 °C. The CNF growths on these samples are presented in Fig. 3. The CNF production when the sample was reduced at 800 °C (M1) is somewhat larger than that observed when the reduction temperature was 700 °C (M2). However, the curve tendencies and their profiles are quite similar suggesting that none of the reduction temperatures (700 or 800 °C) significantly modified the number of the active metallic sites on the Co-Mor surface. This evidence is in clear agreement with the reducibility of the Co species present on the substrate determined by TPR (Fig. 2). To reduce the $Co^{2+}$ located at exchange sites of the mordenite structure, temperatures higher than 800 °C are needed.

As the Co-Mor/Cor reduced at 700 °C was in contact with a mixture reacting stream in which 5% of $H_2$ was added (M3), the initial reaction rate was somewhat higher and the saturation tendency at 175 min was not observed in comparison to the behavior of M2 (Fig. 3). These differences were due to the presence of $H_2$, which was capable of removing the encapsulating carbon deposited over the active metallic sites, thus allowing those sites to produce CNF again. Therefore, $H_2$ acted as a regenerator of the active sites in reaction time.

Fig. 4 shows the reaction rate of CNF production over Co-Mor/Cor reduced at (i) 800 °C (M1), (ii) 700 °C (M2) and (iii) 700 °C and $H_2$ added to its reacting stream (M3). The addition of $H_2$ prevents the formation of encapsulating coke. As a consequence, a decrease in the deactivation rate is observed, the catalyst reaching a higher residual activity.

The CNF growths over calcined Co-Mor/Cor are shown in Fig. 5. Then, the regenerator effect of adding 5% of hydrogen in the reacting stream is again observed (compare the profiles of M4 and M5 with that of M6). On the other hand, the position of the monolith channel path, parallel and perpendicular with respect to the reacting stream direction did not produce any significant changes in the CNF growth. This is concluded if the initial profile and the tendency of the CNF production are compared, first when the sample was placed with its channel paths perpendicular to the reacting flow (M4), and then when the sample was placed with its channel paths parallel to the flow (M5).

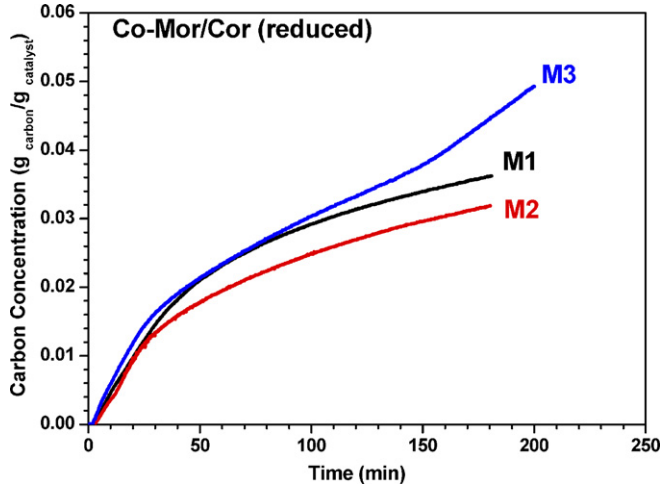


Fig. 3. CNF growth on Co-Mor/Cor reduced at: 800 °C (M1), 700 °C (M2) and 700 °C (M3). Reactant composition: $C_2H_2$ (5%) for M1 and M2 and $C_2H_2$ (8%) + $H_2$ (5%) for M3.

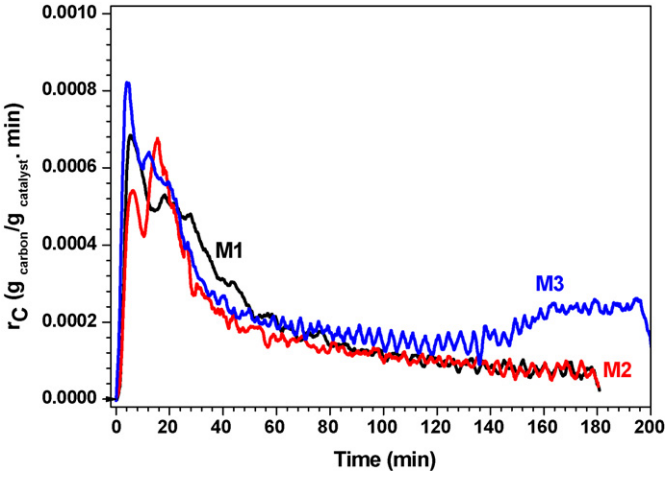


Fig. 4. CNF growth rate at 700 °C on Co-Mor/Cor reduced at: 800 °C (M1), 700 °C (M2) and 700 °C (M3). Reactant composition: $C_2H_2$ (5%) for M1 and M2 and $C_2H_2$ (8%) + $H_2$ (5%) for M3.

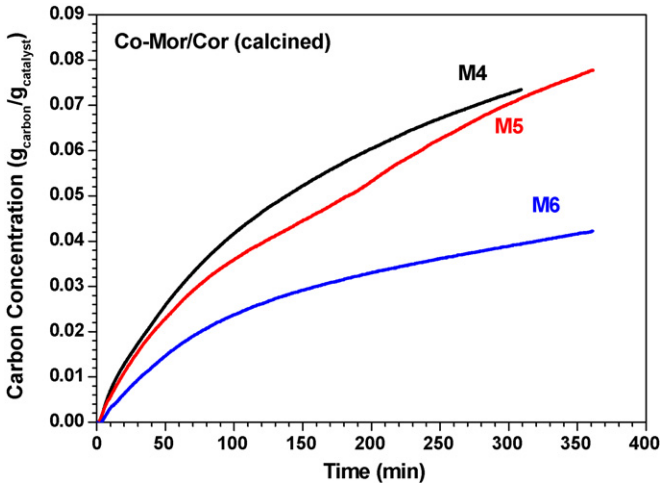


Fig. 5. CNF growth on calcined Co-Mor/Cor. Reactant composition: $C_2H_2$ (8%) + $H_2$ (5%) for M4 and M5, and $C_2H_2$ (5%) for M6. Monolith channel position related to the reacting flow direction: perpendicular (M4) and parallel (M5 and M6).

### 3.3. CNF coating characterization

Figs. 6–8 show the SEM micrographs of CNF produced over M4 (calcined Co-Mor/Cor) at 700 °C using a mixture reacting flow of $C_2H_2$ (5%) and $H_2$ (5%) in $N_2$ balance.

A homogeneous coating of CNF over the substrate walls can be observed, the layer thickness being around 20 μm (Fig. 6). The surface irregularities are due to the mordenite microcrystals. A closer view of this surface Figs. 7 and 8 reveals that the carbon nanofibers form an open pattern. In addition, the rigorous reaction conditions for CNF growth did not affect the stability and the adhesion of the mordenite coating onto the cordierite monolith [3]. Besides, the carbon nanofiber stability is worth noticing since in order to obtain the SEM micrographs, the sample must be cut through its channels.

The XRD patterns of these samples (results not shown) presented the characteristic signals of mordenite and cordierite phases and a weak peak at $2\theta = 26^\circ$, which may be assigned to the [0 0 2] face of graphitic phase [6].

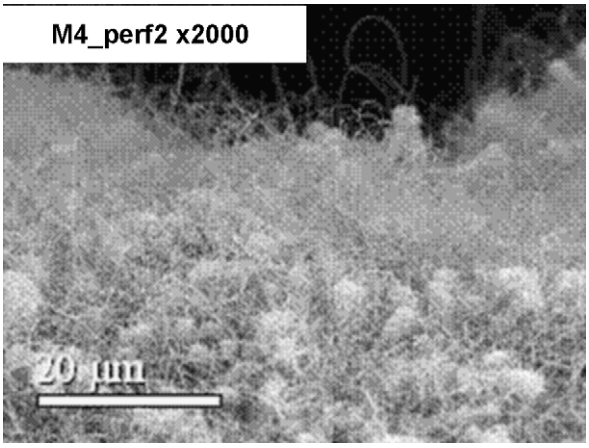


Fig. 6. Morphology of the CNF coating.

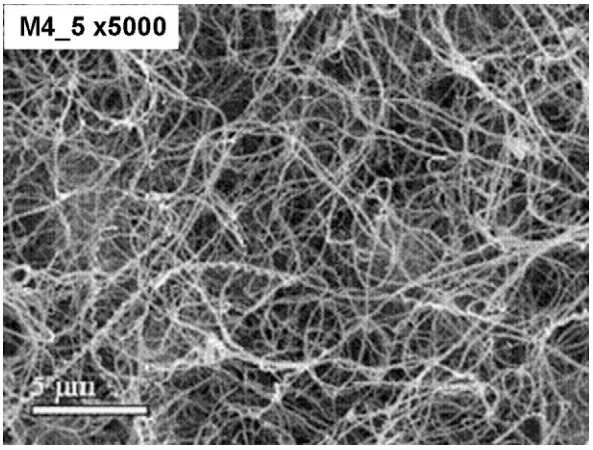


Fig. 7. Open network among the carbon nanofibers.

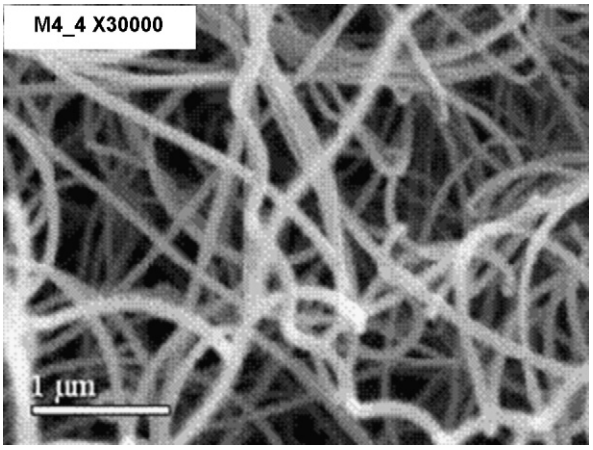


Fig. 8. Morphology of carbon nanofibers.

The Raman spectrum of the CNF coating onto Co-Mor/Cor (M4) is shown in Fig. 9a, where that of the calcined Co-Mor/Cor is also included for the sake of comparison (Fig. 9b). The subtraction of both spectra is presented in Fig. 10. The two typical signals of carbon nanofiber at 1340 and 1592 $cm^{-1}$ are detected. The former signal is assigned to the defect mode, $A_{1g}$ (signal D) and the latter is associated with graphite, mode $E_{2g}$ (signal G). This signal usually has a shoulder at 1620 $cm^{-1}$ due to a maximum of the fonon state density [7].

The integrated intensity ratio of these two signals, D and G, in the Raman spectrum is related to graphite crystallite size ($L_n$) according to [7,8]:

$$L_n\,(\mathrm{nm}) = \frac{4.4}{R} \quad \text{where } R = \frac{I_D}{I_G}$$

The value of $L_n$ for the CNF obtained in our studies is 1.83 nm.

Considering now that both signals have similar extinction coefficients ($\varepsilon_D \sim \varepsilon_G$), it is possible to get the graphitic fraction. The equation is [8]:

$$X_G = \frac{I_G}{I_G + I_D} = \frac{1}{1 + R}$$

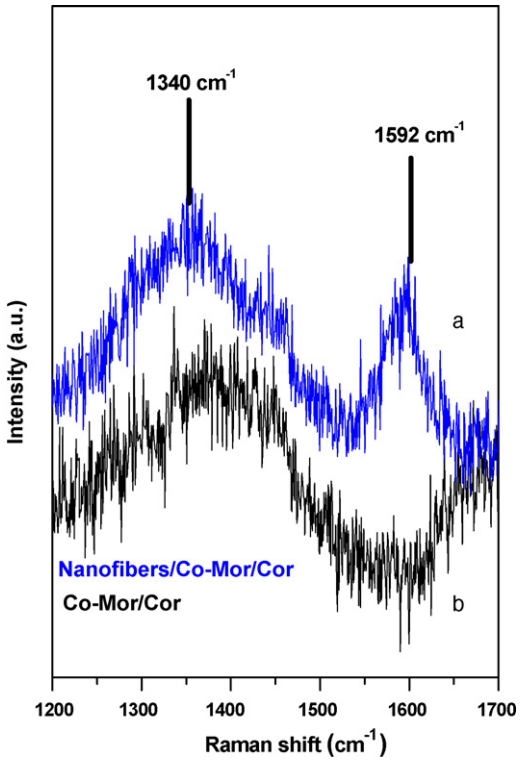


Fig. 9. Raman spectra of: (a) CNF coating on Co-Mor/Cor and (b) Co-Mor/Cor.

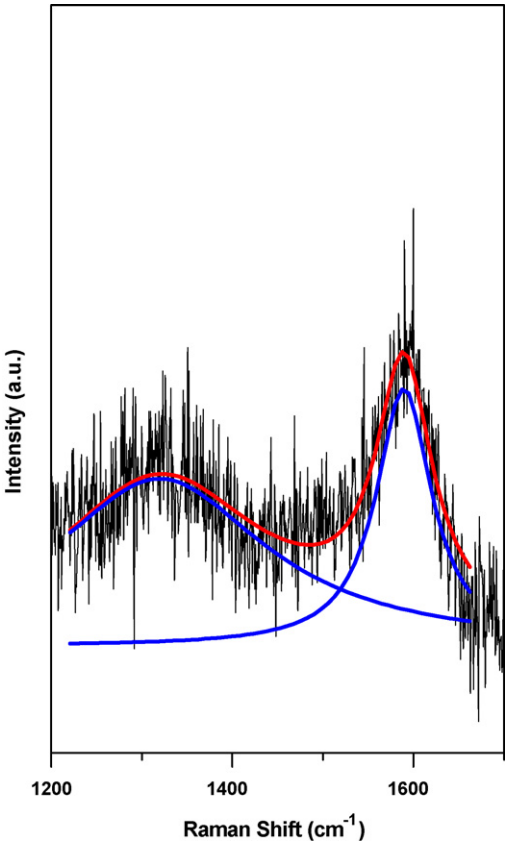


Fig. 10. Spectrum subtraction between CNF coating on Co-Mor/Cor and its substrate (Co-Mor/Cor).

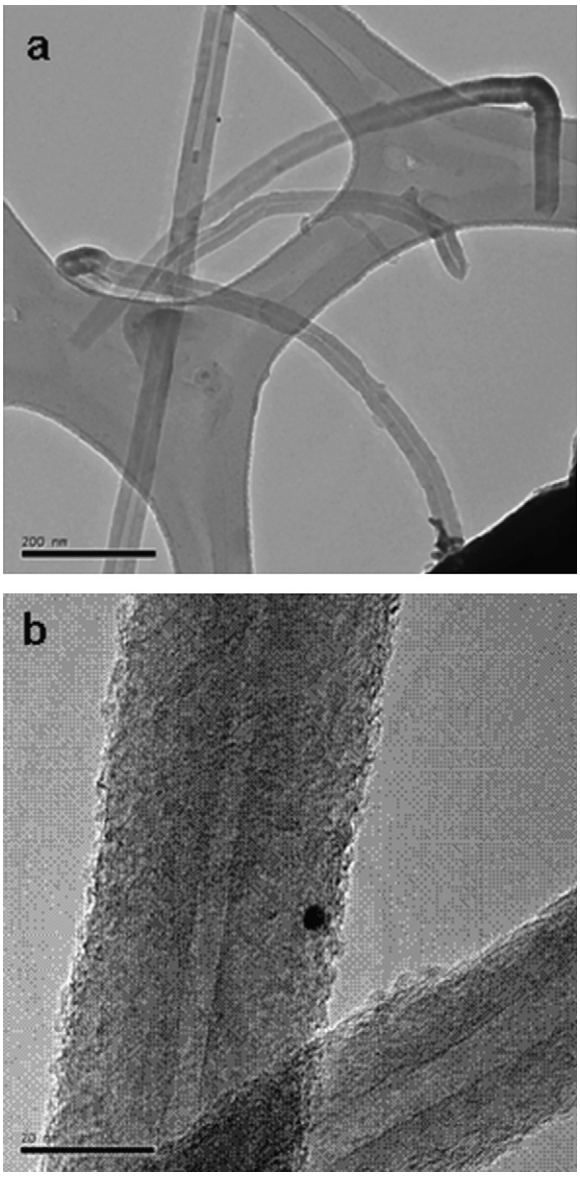


Fig. 11. (a) TEM micrograph of carbon nanofiber growth onto Co-Mor/Cor and (b) a magnification of (a).

The graphitic fraction in M4 is $X_G = 0.35$. This value of $X_G$ is due to the presence of surface defects at the external surface of the carbon nanofibers formed during the decomposition of acetylene.

The TEM micrographs for sample M4 are shown in Fig. 11a and b. The kind of carbonaceous material produced is hollow fiber with multiple walls and a diameter of 40–50 nm. During the reaction (reduced atmosphere), the cobalt interaction decreases with the mordenite structure favoring the $Co^0$ sintering. For this reason, the active metallic particles are larger and the end result is thick fibers.

## 4. Conclusion

The catalytic decomposition of $C_2H_2$ over Co-mordenite coating onto cordierite monolith is a feasible route to obtain carbon nanofiber growth onto this substrate. The stability and

adherence of mordenite to the cordierite walls remain the same after being treated under rigorous reaction conditions.

Under specific operating conditions, it is possible to obtain a stable 20 μm coating of carbon nanofibers onto the Co-Mor/Cor, which increases the specific surface area indicating the potential use of this structured catalyst as a three-phase reactor.

The addition of hydrogen to the reacting stream decreases the catalyst deactivation due to its regenerating effect. The presence of $H_2$ during the reaction keeps the active metallic sites clean, removing the encapsulating carbon deposits.

Concerning the position of the monolith channel path, parallel or perpendicular, with respect to the reacting flow direction, no significant change on the CNF yield was observed.

Hollow fibers with multiple walls and a diameter of 40–50 nm were the carbonaceous material produced under the operation conditions used in this work.

Reducing the Co-Mor/Cor at either 700 or 800 °C did not have any significant influence on the metallic particle size and, consequently, on the CNF diameters. In general, the metallic particle reduction led to a decrease of the cobalt–mordenite structure interaction thus favoring the Co sintering, so that bigger particles were formed producing thick fibers.

Further research is needed on the improvement of metallic particle dispersion by the addition of catalytic and structural modifiers so as to avoid the sintering process. This research path would eventually lead to obtaining fibers with smaller diameters.

## Acknowledgements

The authors wish to acknowledge the financial support received from Ministerio de Educación y Ciencia of Spain (MEC), Project: CTQ 2004-03973/PPQ and from AECI-PIC 2006 program. MAU and VGM thank ANPCyT and Banco Río-Universia 2004. Thanks are also given to Elsa Grimaldi for the English language editing.

## References

[1] N. Jarrah, J.G. van Ommen, L. Lefferts, Catal. Today 79 (2003) 29.
[2] M.T. Kreutzer, F. Kapteijn, J.A. Moulijn, Catal. Today 111 (2006) 111.
[3] M.A. Ulla, E.E. Miró, R. Mallada, J. Coronas, J. Santamaría, Chem. Commun. (2004) 528.
[4] L.B. Gutierrez, E.A. Lombardo, J.O. Petunchi, Appl. Catal. A 194/195 (2000) 169.
[5] C. Resini, T. Montanari, G. Bagnasco, M. Turco, G. Busca, F. Bregani, M. Notaro, G. Rocchini, J. Catal. 214 (2003) 179.
[6] C. Singh, T. Quested, C.B. Boothroyd, P. Thomas, I.A. Kinloch, A.I. Abou-Kandil, A. Windle, J. Phys. Chem. 106 (2002) 10915.
[7] F. Tuinstra, J.L. Koenic, J. Chem. Phys. 53 (1970) 1126.
[8] Y. Wang, S. Serrano, J.J. Santiago-Avilés, Synth. Met. 138 (2003) 423.